*Jurnal Teknologi*, 49(D) Dis. 2008: 27–43


# ESTIMATION OF THE WHEEL-RAIL CONTACT PARAMETERS FOR A CONICAL SOLID-AXLE RAILWAY WHEELSET USING LINEAR INTEGRAL FILTER METHOD

HAZLINA SELAMAT[1], RUBIYAH YUSOF[2] & ROGER M. GOODALL[3]

**Abstract.** This paper addresses the specific problem of estimating the 'conicity' and 'creep coefficients' values of a conical railway wheelset, which vary significantly as the vehicle runs along straight tracks with lateral irregularities. The performances of the continuous-time (C-T) least-squares error (LSE), least-absolute error (LAE) and least-absolute error with variable forgetting factor (LAE+VFF) estimators that employ the linear integral filter (LIF) method are compared. Each estimator was designed based on the fifth order model of a single solid-axle wheelset suspended to ground via lateral springs and dampers connected in parallel. For each simulation, the LAE + VFF estimator performed the best because the algorithm combines the least-absolute error identification that has an instrumental variable element to overcome estimation bias problem and the variable forgetting factor for fast tracking and smooth steady-state estimation. The estimator was then directly applied to a $14^{th}$-order two-axle railway vehicle system where two separate fifth order wheelset model estimators were used to estimate the front and rear wheelsets parameters independently. Since the vehicle body of the two-axle vehicle was effectively decoupled from its wheelsets, the LAE + VFF estimator produced similar estimated front and rear wheelset parameters values, and hence simplifying the estimation process of the more complex 2-axle railway vehicle model.

*Keywords:* Solid-axle; conical wheelset; continuous-time estimation; linear integral filter; least-absolute error; variable forgetting factor

**Abstrak.** Kertas kerja ini membincangkan penganggaran nilai '*conicity*' dan '*creep coefficient*' bagi set roda kereta api berbentuk kon yang mengalami perubahan nilai yang signifikan apabila bergerak di atas landasan lurus yang mempunyai ketaksekataan sisian. Perbandingan prestasi penganggar *least-squares error* (LSE), *least-absolute error* (LAE) dan *least-absolute error with variable forgetting factor* (LAE+VFF) masa selanjar (C-T) dibuat. Setiap penganggar direka bentuk berdasarkan model tertib ke-5 roda kereta api yang disambung ke bumi melalui spring dan peredam sisi. Bagi setiap simulasi, penganggar LAE+VFF memberi prestasi terbaik kerana algoritma ini menggabungkan penganggar *least-absolute error* yang mempunyai elemen *instrumental variable* (IV) bagi menyelesaikan masalah bias dalam penganggaran dan *variable forgetting factor* yang menghasilkan penganggaran dengan penjejakan cepat dan keadaan mantap yang lebih licin. Penganggar ini kemudiannya digunakan terus pada setiap roda sistem kereta api dua gandar bertertib 14. Memandangkan gerabak kereta api ini secara efektifnya boleh dikatakan tidak

[1] Electrical Eng. Faculty, Universiti Teknologi Malaysia, 81310 UTM Skudai, Johor Bahru, Malaysia
Email: hazlina@fke.utm.my
[2] Universiti Teknologi Malaysia, Jalan Semarak, 54100 Kuala Lumpur, Malaysia
Email: rubiyah@citycampus.utm.my
[3] Electrical & Electronics Eng. Dpt., Loughborough University, Leicestershire LE11 3TU, United Kingdom
Email: r.m.goodall@lboro.ac.uk

terganding dengan set roda, penganggar LAE+VFF menghasilkan nilai anggaran yang hampir sama bagi kedua-dua set roda hadapan dan belakang. Ini membolehkan proses penganggaran parameter set roda bagi model kereta api dua gandar yang lebih kompleks di permudahkan.

*Kata kunci:* Bergandar pejal; roda berbentuk kon; penganggaran masa selanjar; penapis terkamir linear; ralat mutlak terkecil; faktor lupaan boleh ubah

## 1.0 INTRODUCTION

Solid-axle wheelset is the most commonly used wheelset on railway vehicles. It consists of two wheels rigidly connected on an axle. The shape of the wheel treads are conical (or otherwise profiled) to allow the wheelset to travel round curves naturally. However, when unconstrained, this type of wheelset suffers from dynamic instability at any speed greater than zero [1]. Furthermore, some of the parameters of the wheelset, namely the 'conicity' ($\lambda$) and 'creep coefficients' ($f_{11}$ and $f_{22}$), are time-varying and their values depend on the wheel-rail profile at the contact point [2]. All of these cause difficulties in the design of the railway vehicle primary suspension system [3].

The wheelset instability can be dealt with using longitudinal spring connections between the wheelset and the bogie/vehicle body, but this interferes with the wheelset's natural curving action. In many research, active control is employed to overcome this design trade-off problem where the springs and dampers of the primary suspension system are replaced or used together with control actuators and other electronic components. Nevertheless, active control with fixed-gain feedback controller may not give satisfactory stability and curving performance when the vehicle is subject to varying $\lambda$, $f_{11}$, and $f_{22}$ values. Therefore, these parameters must be estimated so that the feedback controller is designed based on the estimated current values of the wheelset parameters, providing better control.

Since the dynamics of the railway wheelset/vehicle systems are usually described in continuous-time (C-T) model and there are various problems associated with estimating C-T systems in discrete-time (D-T) [4], linear integral filter (LIF) approach [5] is employed in the parameter estimation process presented in this paper. This is because it allows the estimation of C-T system in D-T without involving any conversion of the system model from C-T to D-T, and vice versa. Moreover, it does not suffer from initial condition problems such as that experienced by, for instance, the algebraic reformulation of transfer function method [6] and numerical integration approach [7].

This paper addresses the specific problem of estimating the wheel-rail contact parameters, which vary significantly as the vehicle runs along straight tracks with lateral irregularities. For this purpose, a self-tuning controller was used in the primary suspension control loop, with the objective of minimizing the wheelset lateral displacement from the track centreline and its yaw angle. The performances of three

parameter estimation algorithms employing the LIF approach, used to estimate the conicity and creep coefficient values, are compared. They are the C-T least-squares error (LSE), least-absolute error (LAE) and least-absolute error with variable forgetting factor (LAE+VFF) estimators.

## 2.0 WHEELSET PARAMETER ESTIMATION

In this paper, only the wheelset with purely coned wheel treads is looked at although in practice, the coned tread has a nonlinear profile with the tread running progressively into the flange. To estimate the time-varying conicity ($\lambda$) and creep coefficients ($f_{11}$, $f_{22}$) values of the conical wheelset, two solid-axle wheelset models were considered: a single solid-axle wheelset suspended to ground via lateral springs and dampers, called Model 1 (Figure 1), and wheelsets on a two-axle railway vehicle system, called Model 2 (Figure 2).

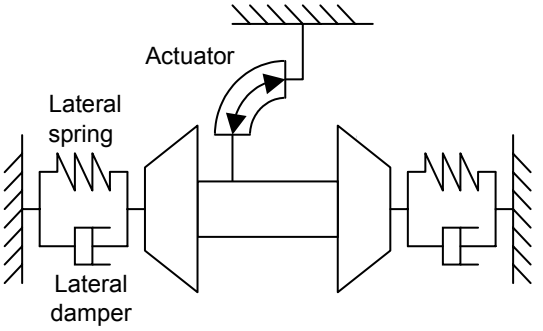


**Figure 1** Model 1 – wheelset suspended to ground

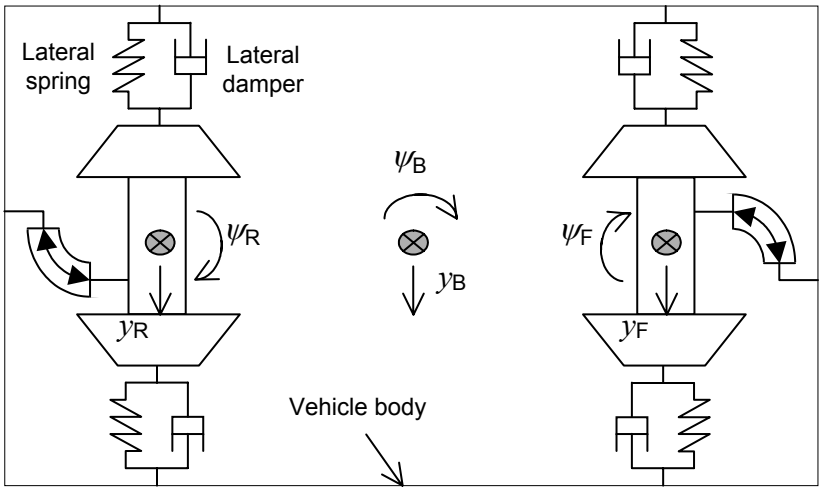


**Figure 2** Model 2 – wheelsets on two-axle railway vehicle

'Conicity' is a term related to the coning of wheel treads and for a pure coned wheelset, its value is equivalent to the coned angle of the tread. 'Creep coefficient' is a term that relates a tangential force acting in a wheel-rail contact patch (known as creep force), with the creepage/creep. It is nonlinearly dependent on the normal force between the wheel and the rail, and the value of this force is changing especially during curving. Other factors such as surface contamination, varying surface condition and railhead shapes can also cause the creep coefficient and conicity values to change. For the wheelset used in the simulation work, it was assumed that all the creep coefficients have the same value and so $f_{11} = f_{22} = f_{wheel}$ was taken. Figure 3 shows the two different variations of $\lambda$ and $f_{wheel}$ values of the conical wheelset used in this paper. Figure 3(a) could represent a wheelset travelling on a piece of railway track to another (possibly new) piece of track, which caused changes in the wheels and track profiles, and hence in the conicity and creep coefficient values. On the other hand, Figure 3(b) represents slowly but continuously varying contact parameter values to simulate, for instance, worn wheels and rail.

The equation of motion of Model 1 and Model 2 are given by Equations (1a–1b) and (2a–2f), respectively [8]. All symbols and typical parameters used are given in the Appendix.

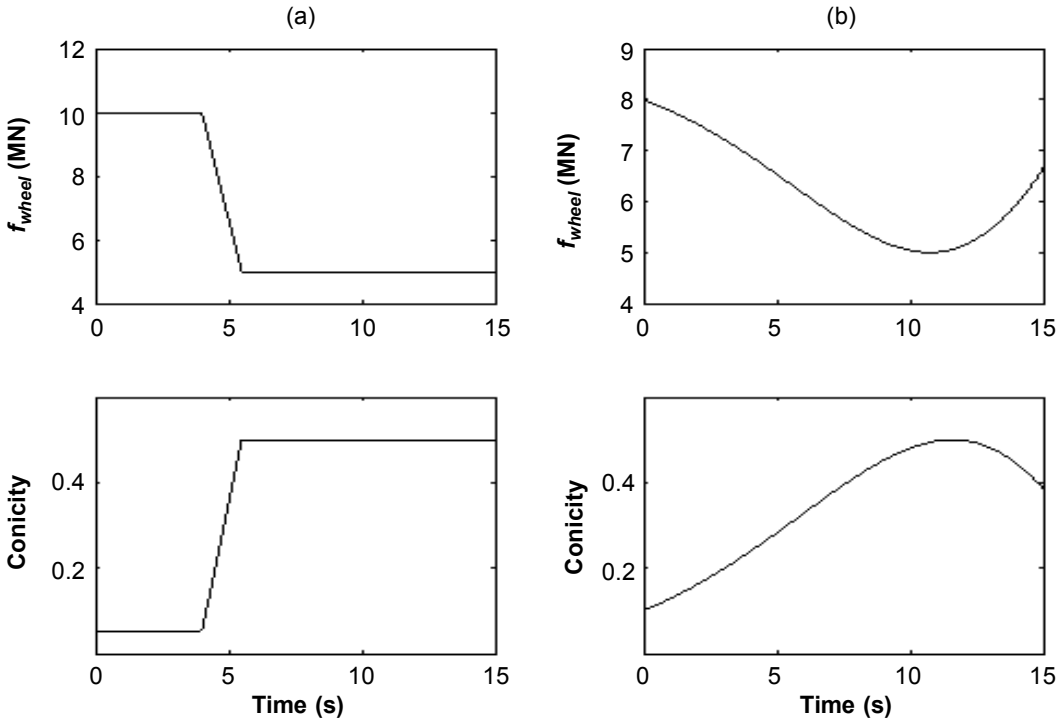


**Figure 3** Time-varying $f_{wheel}$ and conicity: (a) Variation A (b) Variation B

$$m\ddot{y} = -\left(\frac{2f_{22}}{v} + C_l\right)\dot{y} - K_1 y + 2f_{22}\psi \tag{1a}$$

$$I\ddot{\psi} = \frac{-2f_{11}l\lambda}{r_o} y - \frac{2f_{11}l^2}{v}\dot{\psi} + \frac{2f_{11}l\lambda}{r_o} y_l + u \tag{1b}$$

$$m\ddot{y}_F = -\left(\frac{2f_{22}}{v} + C_l\right)\dot{y}_F - K_1 y_F + 2f_{22}\dot{\psi}_F + C_l\dot{y}_B + K_l y_B + C_l l_B\dot{\psi}_B \tag{2a}$$
$$+K_l l_B\psi_B + \frac{mv^2 + 2f_{22}l_B}{R_F} - mg\theta_{cF}$$

$$I\ddot{\psi}_F = \frac{-2f_{11}l\lambda}{r_o} y_F - \frac{2f_{11}l^2}{v}\dot{\psi}_F + \frac{2f_{11}l\lambda}{r_o} y_{lF} + u_F + \frac{2f_{11}l^2}{R_F} \tag{2b}$$

$$m\ddot{y}_R = -\left(\frac{2f_{22}}{v} + C_l\right)\dot{y}_R - K_1 y_R + 2f_{22}\dot{\psi}_R + C_l\dot{y}_B + K_l y_B + C_l l_B\dot{\psi}_B \tag{2c}$$
$$-K_l l_B\psi_B + \frac{mv^2 + 2f_{22}l_B}{R_R} mg\theta_{cR}$$

$$I\ddot{\psi}_R = \frac{-2f_{11}l\lambda}{r_o} y_R + \frac{2f_{11}l\lambda}{r_o} y_{lR} - \frac{2f_{11}l^2}{v}\dot{\psi}_R + u_R + \frac{2f_{11}l^2}{R_R} \tag{2d}$$

$$m_B\ddot{y}_B = C_l\dot{y}_F + K_l y_F + C_l\dot{y}_R + K_l y_R - 2C_l\dot{y}_B - 2K_l y_B \tag{2e}$$
$$+\frac{m_B v^2}{2}\left(\frac{1}{R_F} + \frac{1}{R_R}\right) - \frac{m_B g}{2}(\theta_{cF} + \theta_{cR})$$

$$I_B\ddot{\psi}_B = C_l l_B\dot{y}_F + K_l l_B y_F + C_l l_B\dot{y}_R + K_l l_B y_R - 2{l_B}^2 C_l\dot{\psi}_B - 2{l_B}^2 K_l\psi_B - u_F - u_R \tag{2f}$$

Rotary actuators were used to replace the longitudinal spring connections and to provide yaw torque for controlling the wheelset. The type of controller used was a self-tuning linear-quadratic regulator (S-T LQR) that used the estimated $\lambda$, $f_{11}$ and $f_{22}$ values in the calculation of its feedback gain matrix.

The wheelset/vehicle were considered to be travelling at 83 m/s (approximately 300 km/h) on straight track with lateral irregularities. The velocity of the random track irregularities has a power spectral density (p.s.d) given by Equation 3 [8].

$$\dot{S}_t = \frac{(2\pi)^2 A_{lat} v^2}{f}\left(\text{in}\frac{\left(\text{ms}^{-1}\right)^2}{\text{Hz}}\right) \tag{3}$$

## 2.1 Linear Integral Filter (LIF) Method

The LIF is a method to estimate continuous-time (C-T) system models without converting the models from continuous- to discrete-time (D-T) or vice versa. The C-T model described by Equation 4 is considered where $p$ is the differential operator, $\frac{d}{dt}$, and $\eta$ is the system disturbance.

$$\begin{aligned}&\left(p^n + a_{n-1}p^{n-1} + a_{n-2}p^{n-2} + \ldots + a_0\right)y(t)\\&\quad = \left(b_m p^m + b_{m-1}p^{m-1} + b_{m-2}p^{m-2} + \ldots + b_0\right)u(t) + \eta(t)\end{aligned} \tag{4}$$

Equation 4 can also be expressed in a regression model form given by Equation 5.

$$y_n(t) = \underbrace{\left[-y_{n-1}(t)\cdots - y(t) \quad u_m(t)\cdots u(t)\right]}_{\varphi_\Delta^T(t)}\underbrace{\left[a_{n-1}\cdots a_0 \quad b_m \cdots b_0\right]^T}_{\theta} \tag{5}$$

where $y_i(t) = \dfrac{d^i y(t)}{dt^i}$, $u_i(t) = \dfrac{d^i u(t)}{dt^i}$

To estimate the parameters contained in $\theta$, derivatives of the possibly noisy input and output signals are needed. To avoid accentuating the noise when differentiating these signals, the dynamical system described by differential equations has to be converted into a system described by algebraic equations [4]. This approach is also known as 'linear dynamic (LD) operation' [9]. In this approach, input and output signals are passed through the linear dynamic operator and the sampled signals of the operator's output can be used directly in the estimation algorithm for discrete-time systems. LIF is one of the manifestations of the LD operation.

To apply the LIF, the derivatives of the signals in Equation (5) are first replaced with the integral of the signals by introducing a finite horizon $n^{\text{th}}$-order integration operator, $\Gamma^n$. Then, multiple integrations over the time interval $[t\text{-}l_f T_s, t)$ are performed on both sides of Equation 5 to give Equation 6. $T_s$ is the sampling period and $l_f$ is called the length factor of the LIF.

$$\Gamma^n y_n(t) = \underbrace{\left[-\Gamma^n y_{n-1}(t)\cdots - \Gamma^n y(t) \quad \Gamma^n u_m(t)\cdots \Gamma^n u(t)\right]}_{\varphi_\Delta^T(t)}\theta + \Gamma^n \eta(t) \tag{6}$$

The C-T multiple integrals in ${\varphi_\Gamma}^T(t)$ in Equation (6) are then replaced with their D-T equivalent using normal method of numerical integration utilizing spline-based interpolation of sampled input and output data [5] by means of operator polynomial, $J_i^n(q^{-1})$, where for the multiple integral of any C-T signal, $x(t)$,

$$\Gamma^n x_i(t) = J_i^n\left(q^{-1}\right)\times(kT_s) \tag{7}$$

where,

$$J_i^n\left(q^{-1}\right) = \frac{a!\,T_s^{n-i}}{(a+n-1)!}\cdot\left[D_{l_f}\left(q^{-1}\right)\right]^{n-i}\cdot N_{a+n-i}\left(q^{-1}\right)\cdot N_b\left(q^{-1}\right)\cdot\left(1-q^{-1_f}\right)^i$$

$$D_{l_f}\left(q^{-1}\right) = 1+q^{-1}+\cdots+q^{-(l_f-1)} = \frac{1-q^{-l_f}}{1-q^{-1}}$$

$q^{-1}$ = unit - delay operator, $k$ = discrete - time index, $T_s$ = sampling period
$i$ = 0,1,...,$n$, where $n$ = system order
$l_f$ = length of the discrete - time integration window (LIF)
$a,b$ = orders of the input and output signal internpolation, respectively

$N_0\left(q^{-1}\right) = N_1\left(q^{-1}\right) \equiv 1, N_b\left(q^{-1}\right) = \sum_{i=0}^{b-1} w_{b,b-1}q^{-1}$ = certain 'normal' polynomial of

degree (b – 1) $w_{b,1} = w_{b,b} = 1, w_{b,j} = (b+1-j)w_{b-1,j-1} + jw_{b-1,j}$

Replacing the time index $kT_s$ in Equation (7) with $k$ only, the discrete-time regression model can be written as

$$y_\Gamma(k) = \varphi_\Gamma^T(k)\theta + \eta_\Gamma(k) \tag{8}$$

where,

$$y_\Gamma(k) = J_n^n\left(q^{-1}\right)y(k)$$

$$\varphi_\Gamma^T(k) = \left[-J_{n-1}^n\left(q^{-1}\right)y(k)\ldots - J_0^n\left(q^{-1}\right)y(k)\,J_m^n\left(q^{-1}\right)u(k)\ldots J_0^n\left(q^{-1}\right)u(k)\right]$$

Finally, the three C-T parameter estimators (LSE, LAE and LAE+VFF) are discretised using rectangular approximation method where the minimization criteria for the methods are given below:

LSE: $$J_{LSE}(\theta) = \frac{1}{2}\int_0^t \mu^{t-\tau}\left[y_\Gamma(\tau) - \varphi_\Gamma^T(\tau)\theta\right]^2 d\tau$$

LAE: $$J_{LAE}(\theta) = \int_0^t \mu^{t-\tau}\left|y_\Gamma(\tau) - \varphi_\Gamma^T(\tau)\theta\right| d\tau, \text{with fixed } \mu$$

LAE+VFF: $$J_{LAE+VFF}(\theta) = \int_0^t \mu^{t-\tau}\left|y_\Gamma(\tau) - \varphi_\Gamma^T(\tau)\theta\right| d\tau, \text{with variable } \mu$$

**Table 1** Summary of LSE, LAE & LAE+VFF estimators

| LSE | LAE | LAE+VFF |
|---|---|---|
| • Calculate prediction error<br>$\varepsilon_k = y_{\Gamma k} - \varphi_{\Gamma k}^T \hat{\theta}_{k-1}$ | • Calculate *a priori* prediction error<br>$\varepsilon_k = y_{\Gamma k} - \varphi_{\Gamma k}^T \hat{\theta}_{k-1}$ | • Calculate *a priori* prediction error<br>$\varepsilon_k = y_{\Gamma k} - \varphi_{\Gamma k}^T \hat{\theta}_{k-1}$ |
| • Generate the estimate<br>$\hat{\theta}_k = \hat{\theta}_{k-1} + \frac{P_{k-1}}{\gamma + \varphi_{\Gamma k}^T P_{k-1} \varphi_{\Gamma k}} \varphi_{\Gamma k} \varepsilon_k$ | • Calculate *a posteriori* prediction error<br>$\tilde{\varepsilon}_k = \varepsilon_k - \frac{1}{\gamma_k} \varphi_{\Gamma k}^T P_{k-1} \operatorname{sgn}(\varepsilon_k)$ | • Decide the value of $\gamma$<br>$\mu = \begin{cases} \mu_1 & \text{if } \lvert\varepsilon_k\rvert > \kappa \\ \mu_2 & \text{if } \lvert\varepsilon_k\rvert \le \kappa \end{cases}$<br>$\gamma_k = \mu^T$ |
| • Update the parameter covariance matrix<br>$P_k = \frac{1}{\gamma}\left[ P_{k-1} - \frac{P_{k-1} \varphi_{\Gamma k} \varphi_{\Gamma k}^T P_{k-1}}{\gamma + \varphi_{\Gamma k}^T P_{k-1} \varphi_{\Gamma k}} \right]$ | • Evaluate IV vector<br>$\xi_k = \begin{cases} \frac{\varphi_{\Gamma k}}{\lvert\tilde{\varepsilon}_k\rvert} & \text{if } \lvert\tilde{\varepsilon}_k\rvert \ge \varepsilon_{\min} \\ 0 & \text{if } \lvert\tilde{\varepsilon}_k\rvert < \varepsilon_{\min} \end{cases}$ | • Calculate *a posteriori* prediction error<br>$\tilde{\varepsilon}_k = \varepsilon_k - \frac{1}{\gamma_k} \varphi_{\Gamma k}^T P_{k-1} \operatorname{sgn}(\varepsilon_k)$ |
| | • Generate the estimate<br>$\hat{\theta}_k = \hat{\theta}_{k-1} + \frac{P_{k-1}}{\gamma + \varphi_{\Gamma k}^T P_{k-1} \xi_k} \xi_k \varepsilon_k$<br>where $\gamma = \mu^T$ and $\mu$ = fixed | • Evaluate IV vector<br>$\xi_k = \begin{cases} \frac{\varphi_{\Gamma k}}{\lvert\tilde{\varepsilon}_k\rvert} & \text{if } \lvert\tilde{\varepsilon}_k\rvert \ge \varepsilon_{\min} \\ 0 & \text{if } \lvert\tilde{\varepsilon}_k\rvert < \varepsilon_{\min} \end{cases}$ |
| | • Update the parameter covariance matrix<br>$P_k = \frac{1}{\gamma}\left[ P_{k-1} - \frac{P_{k-1} \xi_k \varphi_{\Gamma k}^T P_{k-1}}{\gamma + \varphi_{\Gamma k}^T P_{k-1} \xi_k} \right]$ | • Generate estimate<br>$\hat{\theta}_k = \hat{\theta}_{k-1} + \frac{P_{k-1}}{\gamma_k + \varphi_{\Gamma k}^T P_{k-1} \xi_k} \xi_k \varepsilon_k$ |
| | | • Update the parameter covariance matrix<br>$P_k = \frac{1}{\gamma}\left[ P_{k-1} - \frac{P_{k-1} \xi_k \varphi_{\Gamma k}^T P_{k-1}}{\gamma + \varphi_{\Gamma k}^T P_{k-1} \xi_k} \right]$ |

Table 1 gives the summary of the estimation algorithms, where subscript $k$ represents the discrete-time index. $\varepsilon_{min}$ in both the LAE and LAE+VFF algorithms is a threshold value used to maintain the values of previous $\hat{\theta}$ and $P$ when the current

generated errors are sufficiently small, whereas $\kappa$ in the LAE+VFF algorithm is a design variable that balances the tracking rate and steady-state smoothness of the parameter estimates. It is also worth noticing that the discretised LAE estimator has a similar recursive representation as in the D-T framework of instrumental variable (IV) estimation scheme known from discrete-time identification literature (e.g. [10]). Also, the variable forgetting factor, $\gamma$, provides faster parameter tracking and smooth steady – state of the estimates by producing time-varying gain matrix, $\frac{P_{k-1}}{\gamma_k + \varphi_\Gamma^T k P_{k-1} \xi_k}$.

## 2.2 Parameter Estimator Design

The design of the C-T parameter estimator was based initially on Model 1, using the wheelset's yaw rate, $\dot{\psi}$, and the control torque input, $u$, as the inputs to the parameter estimator. With $\dot{\psi}$ taken as the measured system output, the transfer function of Model 1 is given by

$$G_1(s) = \frac{b_4 s^4 + b_3 s^3 + b_2 s^2}{s^5 + a_4 s^4 + a_3 s^3 + a_2 s^2 + a_1 s + a_0} \tag{9}$$

where, $b_4 = \frac{1}{I}$, $b_3 = \left(\frac{2f_{22}}{mv} + \frac{C_l}{m}\right)\left(\frac{1}{I}\right)$, $b_2 = \left(\frac{K_l}{m}\right)\left(\frac{1}{I}\right)$, $a_4 = \frac{2f_{22}}{mv} + \frac{C_l}{m} + \frac{2f_{11}l^2}{Iv}$,

$a_3 = \frac{K_l}{m} + \left(\frac{2f_{22}}{mv} + \frac{C_l}{m}\right)\left(\frac{2f_{11}l^2}{Iv}\right)$, $a_2 = \left(\frac{K_l}{m}\right)\left(\frac{2f_{11}l^2}{Iv}\right)$, $a_1 = \left(\frac{2f_{11}l\lambda}{Ir_o}\right)\left(\frac{2f_{22}}{m}\right)$,

$a_0 = 0$

Equation 9 was then rearranged into a regression model form (Equation 8) for the purpose of estimating parameters using LIF.

$$y_\Gamma(k) = \varphi_\Gamma^T(k)\theta(k) + \text{estimation error} \tag{10}$$

where,

$$y_\Gamma(k) = J_5^5\left(q^{-1}\right) y_1(k)$$

$$\varphi_\Gamma^T(k) = \left[-J_4^5\left(q^{-1}\right) y_1(k) \ldots - J_0^5\left(q^{-1}\right) y_1(k)\; J_4^5\left(q^{-1}\right) u_1(k) \ldots J_2^5\left(q^{-1}\right) u_1(k)\right]$$

$$\theta(k) = \left[a_4 \ldots a_0\; b_4 \ldots b_2\right]^T$$

The coefficients of the system's transfer function ($a_4$ to $b_2$) in $\theta$ above were estimated. The estimates of $f_{11}$, $f_{22}$ and $\lambda$, i.e. $\hat{f}_{11}$, $\hat{f}_{22}$, $\hat{\lambda}$ were then calculated from any suitable combinations of these estimated coefficients.

The pair $\{ f_s = \frac{1}{T_s} = 300 \text{ Hz}, l_f = 3\}$ was chosen as it gives the LIF a frequency response that lies almost exactly between the least stable (with $f_{11} = f_{22} = 5$ MN, $\lambda = 0.05$) and the most stable (with $f_{11} = f_{22} = 10$ MN, $\lambda = 0.5$) wheelset system's frequency bands.

Two separate estimators, which were identical to that used for Model 1, were used to estimate the front and rear wheelsets parameters of Model 2 independently. Each estimator assumed the estimation of a 5th order transfer function model of the wheelset (Model 1). Therefore, instead of estimating a 14th order model of the two-axle vehicle, two 5th order wheelset models were considered. This simplified the parameter estimation process, but still provided satisfactory results because of the low vehicle body's natural frequencies compared to the wheelset's kinematic frequencies i.e the body is effectively decoupled from the wheelsets. The input signals to the front and rear wheelset estimators were $\{\dot{\psi}_F(t), u_F(t)\}$ and $\{\dot{\psi}_R(t), u_R(t)\}$ respectively. The estimated parameters were supplied to the LQR design algorithm to calculate the controller feedback gain for the two-axle vehicle model.

## 2.3 Self-Tuning Linear Quadratic Regulator (S-T LQR)

The railway wheelset and vehicle systems given by Equations 1 and 2 were arranged in a state space form (Equation 11) so that for Model 1, $\underline{x} = \left[\dot{y}\ y - y_t\ \dot{\psi}\ \psi\ y_t\right]^T$, and for Model 2, $\underline{x} = \left[x_{2F}\ x_{2R}\ x_{2B}\ y_{tF}\ y_{tR}\right]^T$ with $x_{2F} = \left[\dot{y}_F\ (y_F = y_{tF})\ \dot{\psi}_F\ \psi_F\right]$, $x_{2R} = \left[\dot{y}_R\ (y_R - y_{tR})\ \dot{\psi}_R\ \psi_R\right]$ and $x_{2B} = \left[\dot{y}_B\ \left(y_B - \frac{y_{tF} + y_{tR}}{2}\right)\dot{\psi}_B\ \psi_B\right]$.

$$\dot{\underline{x}}(t) = \hat{A}(t)\underline{x}(t) + \hat{B}(t)u(t) \tag{11}$$

$\hat{A}$ and $\hat{B}$ are the estimated system and input matrices respectively, obtained from Equations 1 and 2 with state vectors as defined above. The estimated values of the creep coefficients and conicity produced by the parameter estimator were used in $\hat{A}$ and $\hat{B}$.

The parameter estimation module employing the parameter estimation algorithms described previously provides the LQR design algorithm, which is a type of optimal controller, with the estimated $\lambda$, $f_{11}$ and $f_{22}$ values. The objective of the LQR was to minimize the lateral deflection of the railway wheelset relative to the track centreline and its yaw angle. Therefore the control law was chosen such that it minimized the following cost function

$$J_{LQ} = \int_0^\infty \left( \underline{y}_{LQ}^T(t)\, Q \underline{y}_{LQ}(t) + u_{LQ}^T(t)\, R u_{LQ}(t) \right) dt \tag{12}$$

where $\underline{y}_{LQ} = \left[ y - y_t \;\; \psi \right]^T$ for a Model 1, or $\underline{y}_{LQ} = \left[ y_F - y_{tF} \;\; \psi_F \;\; y_R - y_{tR} \;\; \psi_R \right]^T$ for Model 2. $Q$ and $R$ are weighting matrices, which have been chosen as follows so that they result in the contribution of each controlled state being roughly equal and satisfactory overall control performance.

Model 1: $Q$ = diag (5, 10), $R = 1 \times 10^{-12}$
Model 2: $Q$ = diag (5, 10, 5, 10), $R$ = diag ($1 \times 10^{-12}$, $1 \times 10^{-12}$)

The control law is given by Equations (13) and (14),

$$u(t) = -K(t)\, \underline{x}(t) \tag{13}$$

$$K(t) = -R^{-1} \hat{B}^T(t) P_r(t) \tag{14}$$

where $K(t)$ is the feedback gain matrix and $P_r(t)$ is obtained by solving the Ricatti equation given in Equation (15).

$$\dot{P}_r(t) = -P_r(t) \hat{A}(t) - \hat{A}^T(t) P_r(t) - Q + P_r(t) \hat{B}(t) R^{-1} \hat{B}^T(t) P_r(t) \tag{15}$$

## 3.0 RESULTS & DISCUSSIONS

To assess the performance of each of the parameter estimators used in the simulation work, the following parameters are defined ($N$ is the total number of samples used in the estimation process and $\rho$ is either $f_{wheel}$ or $\lambda$):

(i) Mean absolute percentage error (MAPE) [11] of $\hat{\rho}$ for the $j^{th}$ test run,

$$\Lambda_{j^{th}} \text{ of } \hat{\rho} = \left( \frac{1}{N} \sum_{i=1}^{N} \frac{|\rho_i - \hat{\rho}_i|}{\rho_i} \right) \times 100\%$$

(ii) Average MAPE of $\hat{\rho}$ for $m$ test runs made for each test condition and in this paper, $m$ = 10.

$$E_m \text{ of } \hat{\rho}\,(\%) = \frac{1}{N} \sum_{j=1}^{m} \left( \Lambda_{j^{th}} \text{ of } \hat{\rho} \right)$$

Firstly, the C-T LSE was used to work out the parameters for the LIF. These parameters were then used in the LAE and LAE+VFF algorithms. The effects of

using different values of $l_f$ and $f_s$ for the C-T LSE estimator are given in Table 2. Note that $p = (n \times l_f) + 1$ is the maximum LIF filter order required. Here, $n$ = system model order of Model 1= 5.

From Table 2, the pair $\{f_s = 300$ Hz, $l_f = 1\}$ gave the worst estimation. $l_f = 6$ gave the best estimation but since $p$ that it required was almost twice that of $l_f = 3$ and the difference in the $E_{10}$ 's were not much, $l_f = 3$ can be considered to be the better choice. Also, too small $f_s$ (e.g. 100 Hz) would prevent the important data from being included in the estimation process whereas too high $f_s$ (e.g. 500 Hz) would include too much high frequencies effect such as the measurement/sensor noise, giving less accurate estimation. Therefore, the combination of $f_s = 300$ Hz and $l_f = 3$ were used throughout this paper.

**Table 2** Effects of $l_f$ and $f_s$ on parameter estimates

| | | $f_s$ = 300 Hz | | | $l_f$ = 3 | | |
|---|---|---|---|---|---|---|---|
| | | $l_f$ | | | $f_s$ (Hz) | | |
| | | **1 ($p$ = 6)** | **3 ($p$ = 16)** | **6 ($p$ = 31)** | **100** | **300** | **500** |
| $E_{10}$ of $\hat{f}_{wheel}$(%) | **Var. A** | 16.97 | 13.54 | 13.63 | 15.61 | 13.54 | 24.61 |
| | **Var. B** | 13.85 | 10.98 | 6.35 | 20.33 | 10.98 | 16.77 |
| $E_{10}$ of $\hat{\lambda}$(%) | **Var. A** | 48.04 | 20.24 | 19.68 | 28.02 | 20.24 | 36.37 |
| | **Var. B** | 31.22 | 27.41 | 17.04 | 23.23 | 27.41 | 32.61 |

**Table 3** Effect of $\varepsilon_{\min}$ for LAE on estimates

| | | $\varepsilon_{\min}$ = 0.8 | $\varepsilon_{\min}$ = 0.08 | $\varepsilon_{\min}$ = 0.008 |
|---|---|---|---|---|
| $E_{10}$ of $\hat{f}_{wheel}$(%) | **Variation A** | 14.24 | 3.92 | 23.39 |
| | **Variation B** | 11.22 | 10.24 | 14.49 |
| $E_{10}$ of $\hat{\lambda}$(%) | **Variation A** | 33.119 | 16.30 | 85.62 |
| | **Variation B** | 29.97 | 23.10 | 75.39 |

For the LAE estimator, Table 3 gives the effect that different $\varepsilon_{min}$ values of the LAE algorithm had on the estimates. It shows that the choice of $\varepsilon_{min}$ is quite crucial. Unsuitable values gave extremely inaccurate estimation results. It turned out that the $\varepsilon_{min}$ value should be closer to the average *a priori* prediction estimation error, obtained by first running the estimator with known and fixed system parameters.

Finally, the performances of all the three estimators are compared in Figures 4 and 5, which show that for Model 1, the LAE estimator gave better parameter tracking and less estimation bias than the LSE estimator. This is as a result of having

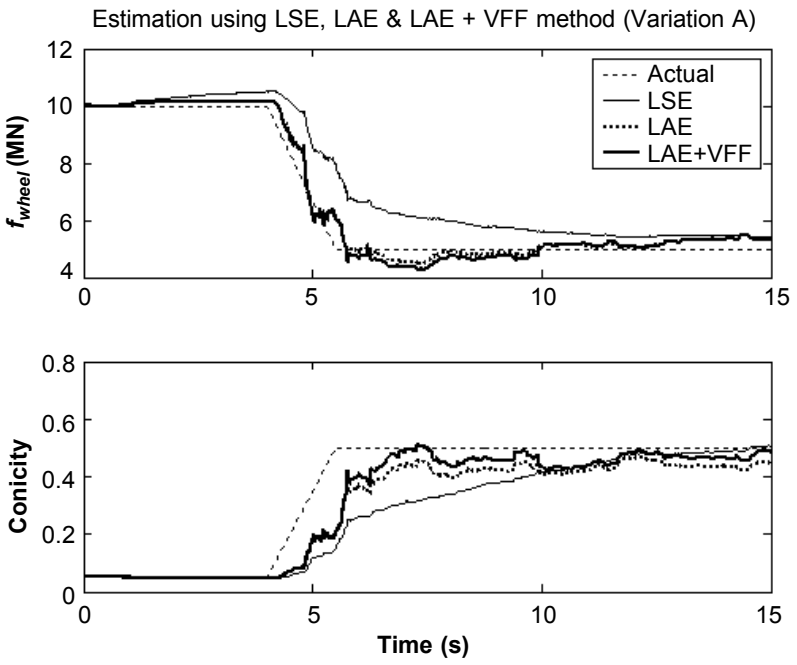


**Figure 4** Comparing the performances of LSE, LAE and LAE + VFF methods – straight track, Variation A

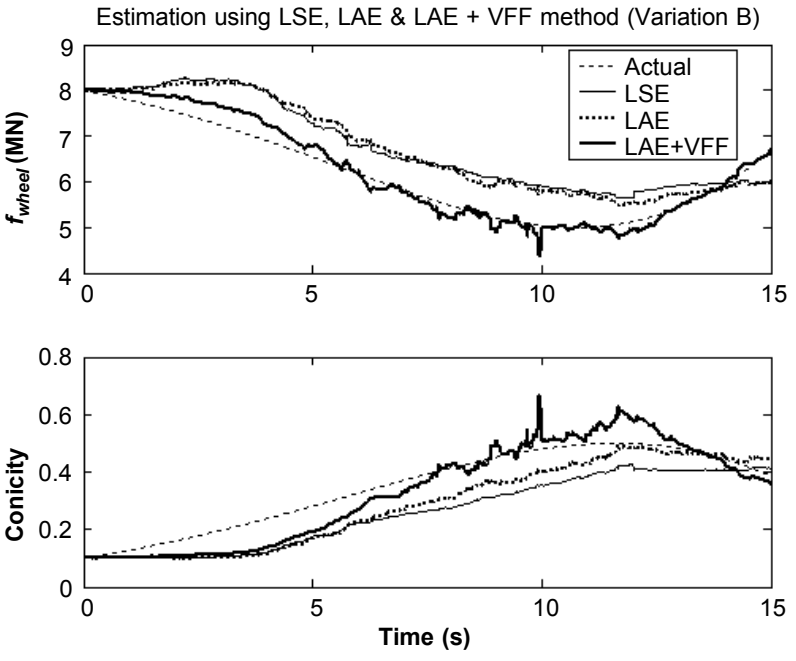


**Figure 5** Comparing the performances of LSE, LAE and LAE + VFF methods – straight track, Variation B

the IV-like element inherent in the algorithm to reduce estimation bias. However, these are further improved when the variable forgetting factor was include in the LAE+VFF estimator. Detailed comparisons are given by Table 4, which again shows that the LAE+VFF estimator was the best of the three and was then used in the estimation of wheelset parameters of Model 2.

Since the estimation results for Variation A and Variation B shown in Table 4 are quite close, only Variation A was considered for the parameter estimation of

**Table 4** LSE, LAE and LAE + VFF methods performances

| | | | **LSE** $\mu = 0.99$ | **LAE** $\varepsilon_{min} = 0.02$ $\mu = 0.99$ | **LAE + VFF** $\varepsilon_{min} = 0.08$ $\kappa = 0.08$ $\mu_1 = 0.8$, $\mu_2 = 0.99$ |
|---|---|---|---|---|---|
| **Var. A** | $\hat{f}_{wheel}$ | $E_{10}$ (%) | 13.54 | 3.92 | 4.90 |
| | | Steady-state error (%) | 8.53 | 7.65 | 7.35 |
| | $\hat{\lambda}$ | $E_{10}$ (%) | 20.24 | 16.30 | 12.31 |
| | | Steady-state error (%) | 5.48 | 10.88 | 3.64 |
| **Var. B** | $\hat{f}_{wheel}$ | $E_{10}$ (%) | 10.98 | 10.24 | 3.84 |
| | $\hat{\lambda}$ | $E_{10}$ (%) | 27.41 | 23.10 | 16.78 |

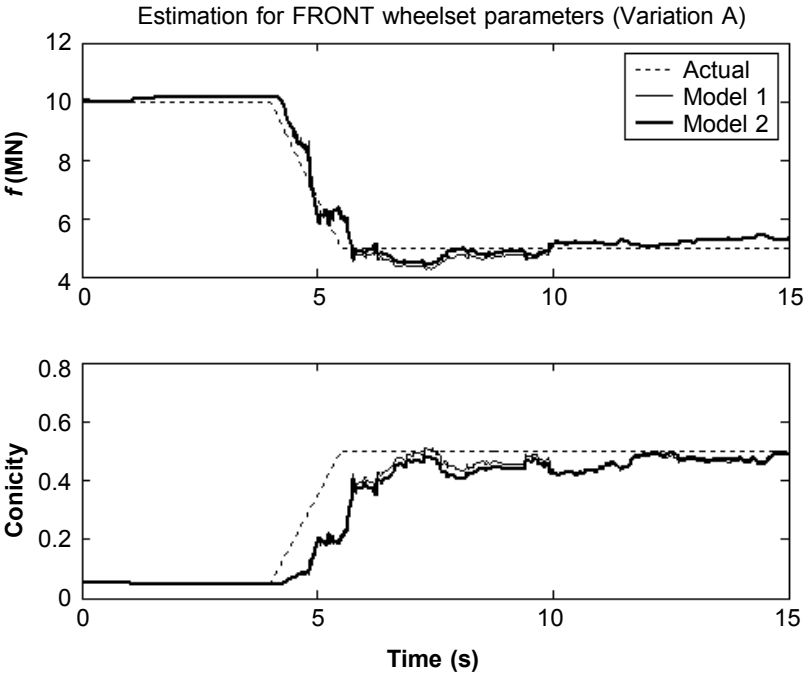

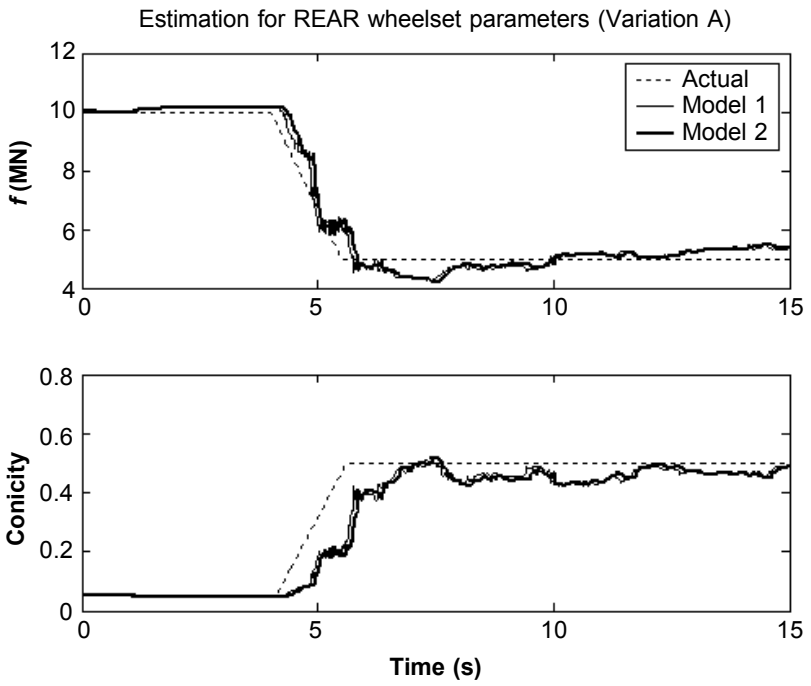


**Figure 6** Comparing parameter estimates of Model 1 and the wheelsets of Model 2

**Table 5** $E_m$ produced by the same LAE + VFF estimator used on Models 1 and 2

| | | On straight track | On curved track |
|---|---|---|---|
| $\hat{f}_{wheel}$ | $E_{10}$ (%) | 4.90 | 4.80 |
| | Steady-state error (%) | 7.35 | 7.29 |
| $\hat{\lambda}$ | $E_{10}$ (%) | 12.31 | 12.24 |
| | Steady-state error (%) | 3.64 | 3.42 |

Model 2. The same LAE + VFF parameter estimator designed for Model 1 was applied to each of the two wheelsets on the two-axle railway vehicle (Model 2), and Figure 6 and Table 5 show that the estimator designed based on Model 1 can be directly used on Model 2 to give similar estimation results.

## 4.0 CONCLUSIONS

In estimating the time-varying wheelset conicity and creep coefficient values, the LIF approach was adopted to avoid problems of estimating continuous-time system parameters in discrete-time, and without suffering from initial condition problem. The effectiveness of three different parameter estimation algorithms utilising the LIF

technique were compared. They were the C-T LSE, LAE and LAE + VFF methods. Each estimator was designed based on the fifth order model of a single conical solid-axle wheelset suspended to ground via lateral springs and dampers connected in parallel. For this wheelset system travelling on a straight track with lateral irregularities, the LAE + VFF estimator performed the best. This is because the LAE + VFF algorithm combines the continuous-time least-absolute error identification that has an IV element to overcome the estimation bias problem and the variable forgetting factor method for fast tracking and smooth steady-state estimation. The LAE+VFF estimator was then directly applied to a two-axle railway vehicle system where two separate fifth order wheelset model estimators were used to estimate the front and rear wheelsets parameters independently. Since the vehicle body of the two-axle vehicle was effectively decoupled from its wheelsets, the LAE + VFF estimator produced similar estimated front and rear wheelset parameters values, and hence simplifying the estimation process of the higher order 2-axle railway vehicle model.

## ACKNOWLEDGEMENT

The authors would like to thank Universiti Teknologi Malaysia and Loughborough University for their support.

## APPENDIX

| Symbol | Parameter |
|---|---|
| $y$, $\psi$ | Lateral displacement and yaw angle of the solid-axle wheelset, respectively |
| $u$ | Control input signal |
| $y_F$, $y_R$, $y_B$ | Lateral displacement of front (leading), rear (trailing) wheelset and vehicle body |
| $\psi_F$, $\psi_R$, $\psi_B$ | Yaw displacement front (leading), rear (trailing) wheelset and vehicle body |
| $v$ | Vehicle travel speed |
| $m$, $I$ | Wheelset mass (1250 kg) and yaw inertia (700 kg m$^2$) |
| $l$, $l_B$ | Half gauge of wheelset (0.7 m) and half space of the vehicle body (4.5 m) |
| $r_o$, $\lambda$ | Wheel radius (0.45 m) and conicity |
| $m_B$, $I_B$ | Vehicle mass (30 000 kg) and yaw inertia (558 800 kg m$^2$) |
| $K_l$, $C_l$ | Lateral stiffness (200 kN/m) and damping (50 kN s/m) per wheelset |
| $f_{11}$, $f_{22}$ | Longitudinal and lateral creep coefficients |
| $R_F$, $R_R$ | Radius of the curved track at the front (leading) and rear (trailing) wheelsets |

| | |
|---|---|
| $\theta c_F$, $\theta c_R$ | Cant angle of the curved track at the front (leading) and rear (trailing) wheelsets |
| $y_{tF}$, $y_{tR}$ | Track lateral displacement (irregularities) at the front (leading) and rear (trailing) wheelsets |
| $u_F$, $u_R$ | Controlled torque input for the front (leading) and rear (trailing) wheelsets |
| $g$ | Gravity (9.8 m/s$^2$) |

## REFERENCES


[1] Knoth, K. and F. Böhm. 1999. History of Stability of Railway and Road Vehicles. *Vehicle System Dynamics*. 31: 283-323.

[2] Pearce, T. G. 1996. Wheelset Guidance – Conicity, Wheel Wear and Safety. *Proc. Instn. Mech. Engnrs.* 210: 1-9.

[3] Goodall, R. M. 1999. Tilting Train and Beyond-the Future of Active Railway Suspensions. Part 1: Improving Passenger Comfort. *Computing & Control Engineering Journal.* August: 153-160.

[4] Wang, L. and P. J. Gawthrop. 2001. On the Estimation of Continuous-time Transfer Functions. *Int. Jnl. Control*. 74(9): 889-904.

[5] Kowalczuk, Z. and J. Kozlowski. 1998. Integrated Squared Error and Integrated Absolute Error in Recursive Identification of Continuous-time Plants. *UKACC Int. Conf. on Control 1998.* September 1-4. 455: 693-698.

[6] Johansson, R. 1994. Identification of Continuous-time Models. *IEEE Trans. on Signal Processing*. 42(4): 887-897.

[7] Whitfield, A. H. and N. Messali. 1987. Integral-equation Approach to System Identification. *Int. Jnl. Control*. 45(4): 1431-1445.

[8] Mei, T. X. and R. M. Goodall. 1999. Optimal Control Strategies for Active Steering of Railway Vehicles. *Proc. IFAC 1999*. Beijing, China. 215-256.

[9] Unbehauen, H. and G. P. Rao. 1990. Continuous-time Approaches to System Identification – A Survey. *Automatica*. 26(1): 23-35.

[10] Young, P. C. 1970. An Instrumental Variable Method for Real-time Identification of a Noisy Process. *Automatica*. 6: 271-287.

[11] Abramowitz, M. and I. Stegun. 1972. *Handbook of Mathematical Functions*. New York: Dover Publications.